Case Studies in Construction Materials 16 (2022) e01054

Contents lists available at ScienceDirect

Case Studies in Construction Materials

journal homepage: www.elsevier.com/locate/cscm

Flexural behavior of HSC beams reinforced by hybrid GFRP bars with steel wires

Taha A. El-Sayed [*,1], Abeer M. Erfan, Ragab M. Abdelnaby, Mohamed K. Soliman

Department of Structural Engineering, Shoubra Faculty of Engineering, Benha University, Egypt

ARTICLE INFO

Keywords:
Flexural performance
Hybrid-GFRP (HGFRP) bars
Nonlinear analysis (NLA)
Glass Fiber Reinforced Polymers (GFRP)
Steel wires
National Building Research Center (NBRC),
Ansys 2019-R1

ABSTRACT

This study offers the flexural performance of HSC beams of 60 MPa compressive strength with locally manufactured hybrid-GFRP (HGFRP) bars with steel wires in experimental and analytical manners. Both investigations were done to explore the influence of using HGFRP bars with various reinforcement ratios for these beams as a new ductile hybrid reinforcement. So, six beams of dimension 150X300X1700 mm were tested in the National Building Research Center-Cairo, Egypt till failure. The main variables were the reinforcement types (steel, GFRP, Hybrid GFRP). The ultimate loads, mid-span deflections, and reinforcement bars strains of the tested beams were documented. Nonlinear analysis was assembled to validate the flexural performance of beams using ANSYS program, in terms of ultimate load, stains, crack pattern and load deflection curves. Numerical investigations good agreement with experimental ones in terms of ultimate loads and deflections, cracking patterns, and the behavior of load deflection.

1. Introduction

The last years, FRP reinforcement bars were utilized as an alternate of steel bars to solve the corrosion. The familiar fibers sorts are glass, carbon, and aramid. More research on the performance of RC beams reinforced by FRP bars were examined [1–6]. Erfan et al. [1] investigated an experimental study for HSC beams reinforced by GFRP bars. The ultimate failure load, ultimate deflection and cracking patterns of the beams were assessed.

FRP is commonly utilized as an alternative material to overcome the corrosion problem of steel reinforcement and to extend the service life of reinforced concrete (RC) constructions. In comparison to steel reinforcement [7] FRP rebar can provide high tensile strength as well as strong corrosion resistance for RC structures, particularly those exposed to corrosive conditions such as sea water. However, because to its low elastic modulus and brittle fracture, FRP has not been widely used as reinforcement or structural materials in civil engineering constructions.

FRP is primarily made up of fibers and resin. Glass and carbon are two popular fiber materials. Carbon fiber outperforms steel in terms of tensile strength and elastic modulus. These are structural advantages of employing carbon fiber, but not economically, because its price is nearly 10 times that of glass fiber. Glass fiber may be a more cost-effective material in the beginning. The biggest disadvantage of employing glass fiber is its low modulus of elasticity, which achieves less than a fourth of the elastic modulus of steel. When FRP rebar is employed as the reinforcement for flexural members, this causes excessive deflection. As a result, the idea of

* Corresponding author.
E-mail address: taha.ibrahim@feng.bu.edu.eg (T.A. El-Sayed).
[1] Official website: http://www.bu.edu.eg/staff/tahaibrahim3

https://doi.org/10.1016/j.cscm.2022.e01054
Received 17 February 2022; Received in revised form 29 March 2022; Accepted 4 April 2022
Available online 6 April 2022

Table 1
Beams details.

Specimen Symbol	RFT. Type	Tension RFT.	Reinforcement ratio μ %	Comp. RFT.	Steel-Wire Number
B1	Steel	2Ø10	0.94	2Ø10	—
B2	GFRP	2Ø10	1.00 μ_b	2Ø10	—
B3	HGFRP	2Ø10	1.40 μ_{fb}	2Ø10	3 wires
B4	HGFRP	2Ø10	1.60 μ_{fb}	2Ø10	5 wires
B5	HGFRP	2Ø12	2.40 μ_{fb}	2Ø10	4 wires
B6	HGFRP	2Ø12	2.60 μ_{fb}	2Ø10	6 wires

* Hybrid GFRP bars with steel wires of 1 mm diameter.
* μ_b: balanced reinforcement ratio

"hybridization" was developed to help FRP rebar overcome its disadvantages. Many scholars have looked on FRP hybridization [8–11].

The most prevalent outcomes of steel reinforcement corrosion include deterioration, reduced serviceability, and failure of concrete buildings reinforced with steel bars. As a result of the significant increase in maintenance and repair expenses, this problem has become a serious worry in the construction sector. Because of their non-corrosive and non-magnetic qualities, FRP has emerged as a creative solution for alternative reinforcement in concrete buildings, making them an appropriate reinforcement for harsh environments and circumstances requiring magnetic transparency. However, due to the low modulus of elasticity of FRP, the flexural stiffness of concrete parts reinforced with FRP bars is significantly reduced. This decrease happens after cracking, resulting in a significant increase in deformation under service conditions [12].

Furthermore, due to the linear-elastic behavior of FRP composite materials up to rupture, continuous concrete beams reinforced with FRP bars have a lower capacity to disperse loads across crucial sections than steel bars [13–16]. As a result, a collapse with little or no warning is predicted. As a result, there is a need for a new way of construction that is robust, cost effective, and ductile to prevent such difficulties. Several ways for improving ductility have been proposed, including hybridization of different types of fibrous material [17–19] and mixing steel reinforcement with composite materials to create rebar with inner steel and an outside FRP [20–24]. Due to the high cost and complexity of the production process, these initiatives were not feasible for implementation in the construction sector. More practical solutions have been proposed, including concrete confinement in the compression zone [25], the addition of fibers to concrete [26–28], and the use of a hybrid mix of FRP and steel bars [18–26]. When compared to traditional reinforcement, this hybrid reinforcement system exhibits better serviceability and ductility, as well as increased load-carrying capability [29–31]. Some studies had used the hybrid bars schemes in reinforced concrete elements [32–40]. Fewer studies connected to study the ability of utilizing steel or FRP at the same time as hybrid reinforcement bars [41–44].

The previous studies were restricted to explore the hybrid bars performance only. So, this study tried to establish the manufacture of the hybrid bars to improve ductility behavior of the RC beams. The hybrid bars properties were assessed. Six RC beams reinforced by hybrid bars were tested. NLA was done to validate the experimental tested RC beams using ANSYS program Ver. 2019-R1 [46].

2. Experimental investigation

The experimental program was done in the National Building Research center (NBRC), Giza, Egypt. Six beams of dimension 150x300x1700 mm were cast and tested under two-point load till failure using a testing machine of 2000kN capacity. The most important objective of this study to get the ultimate loads, deflections, strains in concrete and HGFRP reinforcement bars and cracks patterns its propagation of all beams. All beams' details are given in Table 1 and Fig. 1.

2.1. Concrete matrix

The concrete mix of 60 MPa compressive strength using cubes (f_{cu}) was used. The concrete mix properties as given in Table 2.

2.1.1. Compressive strength test

On cube samples of 150 ×150 x 150 mm, a compressive strength test was performed. After 28 days, the samples were tested. The testing was carried out using universal testing equipment with a capacity of 2000kN, as shown in Fig. 2. The compressive strength of the three tested cubes was calculated as shown in Table 3.

2.2. Hybrid-GFRP bars

The aim for using Hybrid-GFRP bars as a repalcement of GFRP bars was to improve boththe GRFP bars elastic modulus and the brittlness to be almost ductile or semi-ductile. These chrachteristics improve the loading-carrying capcities of the RC-beams reinforced by Hybrid-GFRP bars. The locally manufactured HGFRP is as shown in Fig. 3 and tested as in Fig. 4. Table 4 showed the tensile strength of all used diamerters for steel, GFRP and the HGFRP bars.

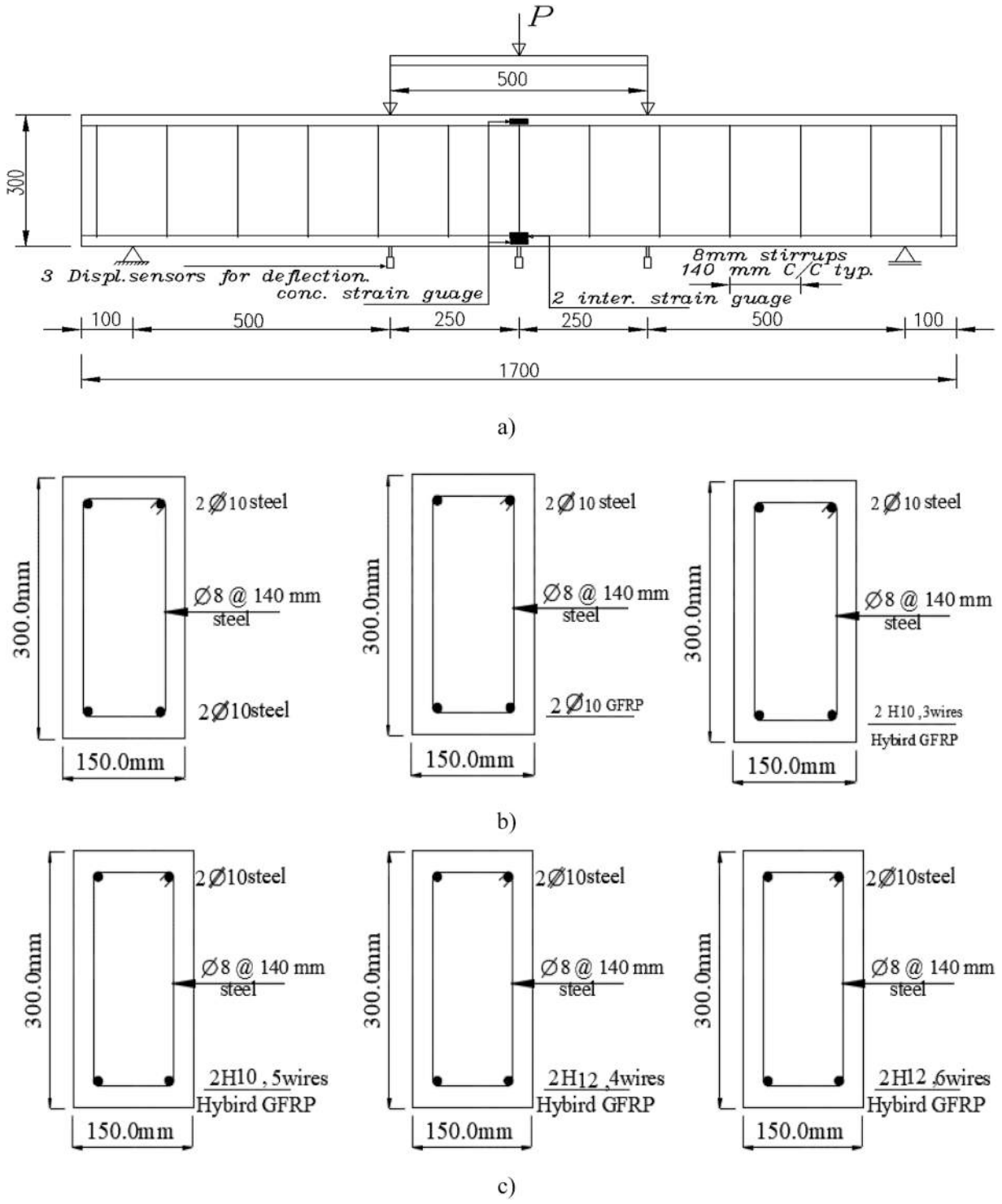

Fig. 1. Typical Beams Geometry and reinforcement details.

Table 2
concrete mix design.

Item	Cement (kg/m^3)	Coarse aggregate (kg/m^3)	Fine aggregate (kg/m^3)	Water (kg/m^3)	Silica Fume (kg/m^3)	Superplasticizer (kg/m^3)
Per m^3 of concrete (60 MPa)	600	1200	600	150	60	20

Fig. 2. Concrete cubes testing.

Table 3
Compressive strength test results.

Cubes	Compressive Strength (MPa) 28 days
Cube-1	63.9
Cube-2	62.2
Cube-3	61.7
Avg.	**62.6**

Fig. 3. Locally produced HGFRP bars.

Fig. 4. HGFRP bars samples for the tensile strength testing of a) pasting strain gauge on bars, b) tensile test for HGFRP bars.

Table 4
Tensile strength and strain for all reinforcement bars.

Reinforcement Type	Diameter (mm)	Yield strength f_y (MPa)	Ultimate Tensile strength f_u (MPa)	Ultimate Strain (mm/mm)
Steel	8.0	240	350	0.00175
Steel	10.0	400	650	0.00325
GFRP	10.0	580	580	0.01360
HGFRP-3wires	10.0	620	620	0.01190
HGFRP-5wires	10.0	670	670	0.01220
HGFRP-4wires	12.0	760	760	0.01210
HGFRP-6wires	12.0	810	810	0.01250

Fig. 5. Testing Set up details.

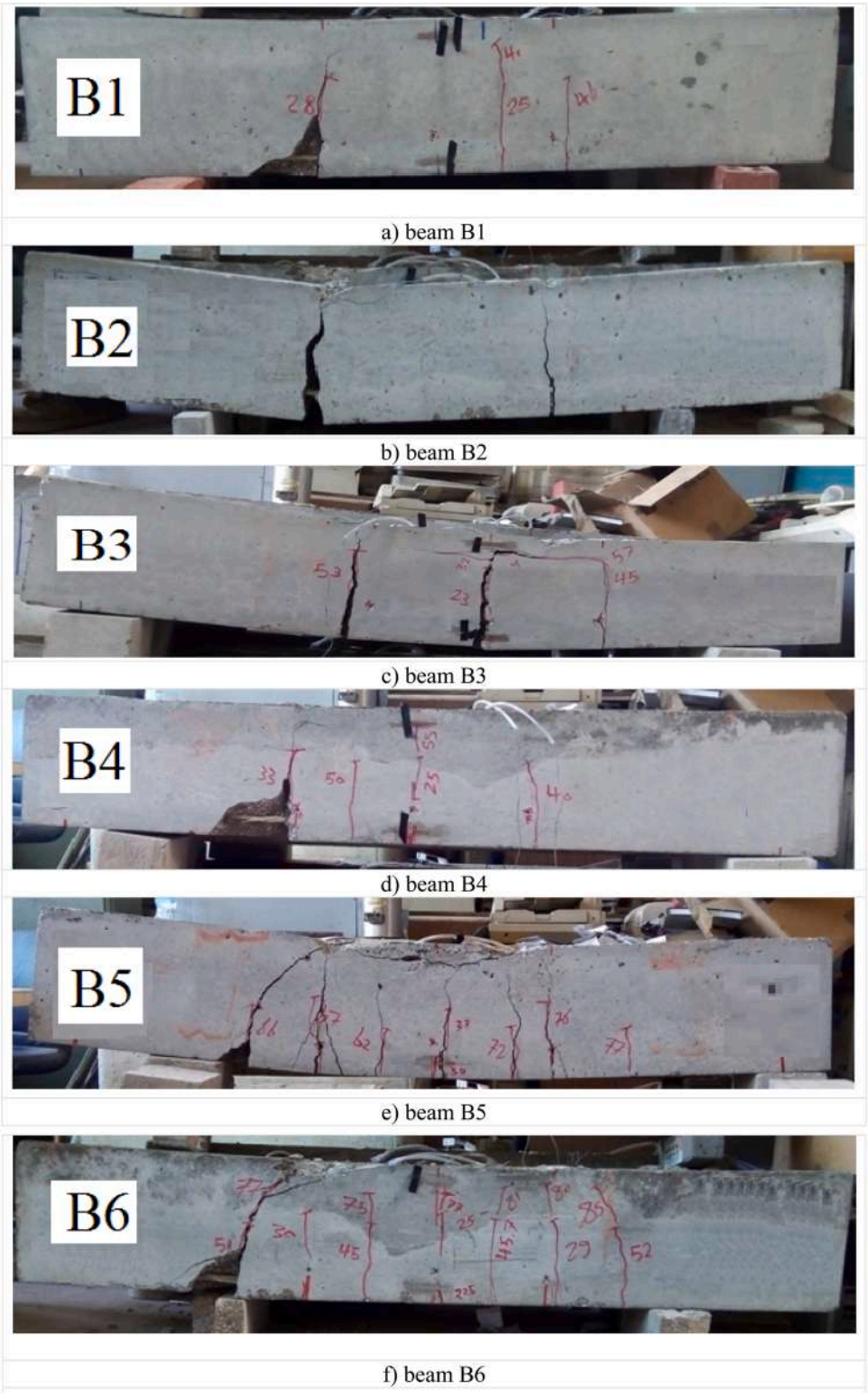

Fig. 6. Crack pattern for all beams.

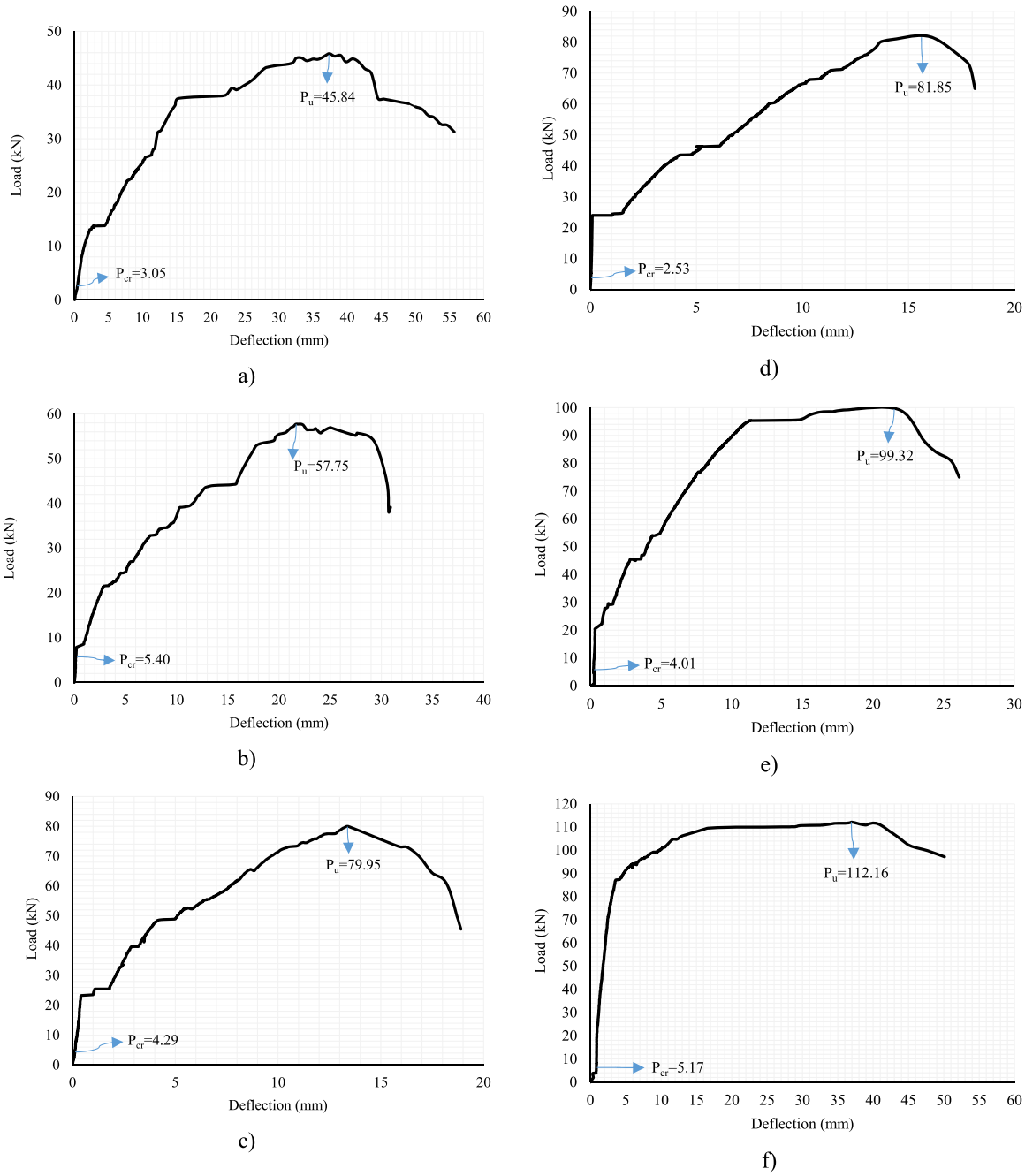

Fig. 7. Experimental load-deflection curve; a) B1; b) B2; c) B3; d) B4; e) B5; f) B6.

2.3. Test setup

All beams were tested under four-point bending testing machine of maximum capacity of 2000kN. Load control was used to test the beams. The beams effective span was 1500 mm and the distance between the two points of applied load was 500 mm as shown in Fig. 5. LVDT was used to measure the deflections at mid span of the tested beams for every 0.5kN load increment. Strain gauges were set at the main reinforcement bars for measuring the bars strain.

Table 5
Experimental ultimate Load.

Specimen Id	First crack load (kN)	Ult. load (kN)	def. at first crack load (mm)	def at ult. load (mm)	Ductility ratio —	Mode of failure
B1	3.05	45.84	0.12	37.35	311.25	F.T.F
B2	5.40	57.75	0.38	22.12	58.21	G.R
B3	4.29	79.95	1.75	13.42	7.67	F.T.F
B4	2.53	81.85	0.14	16.00	114.29	F.T.F
B5	4.01	99.32	0.62	21.82	35.20	F.T.F
B6	5.17	112.16	0.27	37.02	137.11	F.T.F

*F.T.F: flexural tension failure. *G.R: GFRP bars rupture. *H-G.R: flexural tension failure.

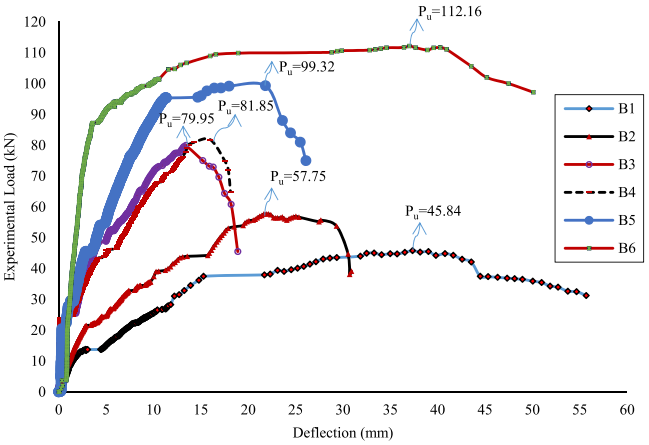

Fig. 8. Experimental load deflection curves for all beams.

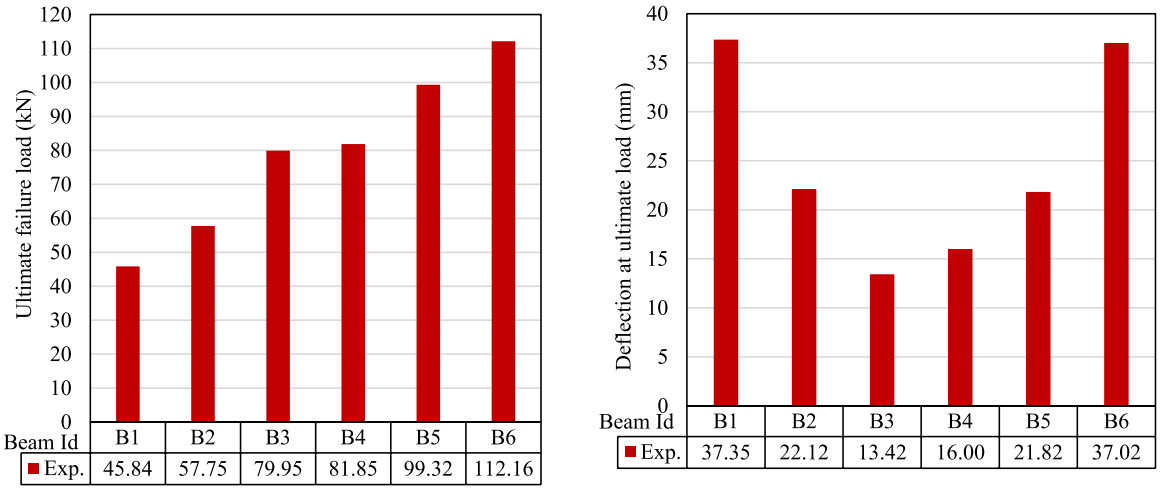

Fig. 9. Comparison between experimental results, a) ultimate load, b) deflection at ultimate load.

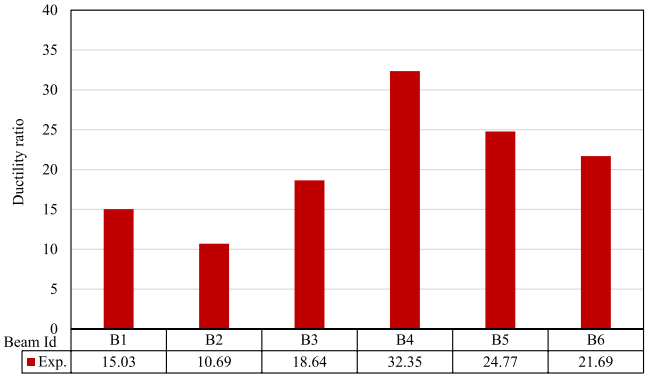

Fig. 10. Ductility ratio.

3. Results and discussion

3.1. Crack pattern

The first cracks appeared in all specimens in the stress zone in the center of the beams. The remaining fractures appeared as tension cracks, as seen in Fig. 6. For sample beams B1 and B2, stress is present, however crack numbers varied. The first crack in B1 was noticed at 3.05 kN, while the first crack in B2 was observed at 5.40 kN. The first fractures develop at 4.29 kN, 2.53 kN, 4.01 kN, and 5.17 kN for beams B3, B4, B5, and B6, respectively, due to the identical process of cracks appearing for the other specimens.

3.2. Experimental load-deflection curves

The load-deflection curves for all specimens investigated are shown in Figs. 7 & 8. As shown in Table 5, samples with higher first crack load deflection had lower failure load deflection and, as a result, a lower index of ductility. Fig. 7 and Table 5 the ultimate loads of hybrid GFRP specimens were greater than those of the control specimen. During the test, the first crack load was only visually observed for all beams.

3.3. Ultimate load and corresponding deflection

Table 5 and Fig. 8 show the ultimate load and its related deflection. The maximum loads for control beams B1 and B2 are 45.84 kN and 57.75 kN, respectively, with deflections of 37.35 mm and 22.12 mm. The ultimate loads for beams B3, B4, B5, and B6 are 45.84 kN, 57.75 kN, 99.32 kN, and 112.16 kN, respectively. Their relative deflections are 13.42 mm, 16.00 mm, 21.82 mm, and 37.02 mm. Fig. 9

3.4. Ductility response

The ductility is defined as the ratio of the ultimate failure loads to the initial crack loads. The ductility of the specimens is shown by the presence of steel or hybrid GFRP reinforcement. The distinction between steel and Hybrid GFRP reinforcement is that Hybrid GFRP has a high degree of ductility. The ductility achieved from specimens reinforced employing Hybrid GFRP bars relates to the high experimental ultimate load to the load of the first fracture. Fig. 10 and Table 5 compare the obtained ductility for each specimen.

3.5. Crack characterization

Table 5 & Fig. 7 show the failure mechanism for each specimen. The steel reinforcement control beam failed in flexure due to steel bar yielding, which resulted in concrete crushing. Tension failure in GFRP reinforcement was defined by the rupture of GFRP bars at the zone of bending moment, which occurred in beam B2 which was reinforced with GFRP ratio equal to the balanced reinforcement ratio μ_b [45]. For H-GFRP beams (B3 to B6), the mode of failure was yielding of H-GFRP bars followed by crushing in concrete before the rupture of Hybrid-GFRP reinforcement, which is similar to flexural tension failure. Fig. 11

4. Non-linear finite element analysis

The concrete beams reinforced with Hybrid GFRP bars were simulated using non-linear finite element analysis. To do this, the ANSYS program [46] was employed. The major parameters that will be covered in the finite element software are ultimate load, deflection, initial cracks, crack patterns, and ductility. As a consequence, there is consistency between the derived NLFEA findings and the experimental data, which validate the ANSYS model. The program for the beams employed in the experimental investigation is the

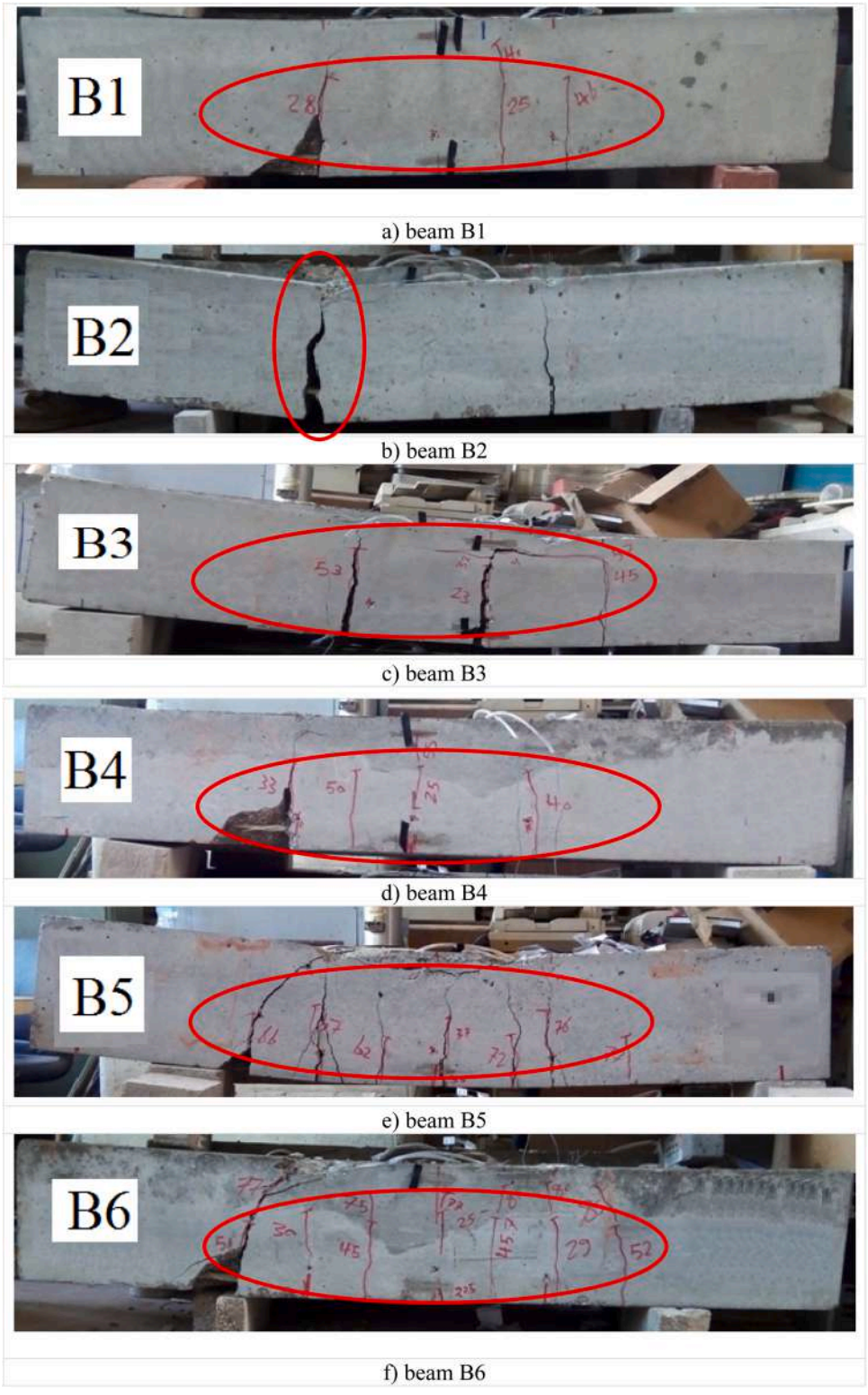

Fig. 11. Crack characterization.

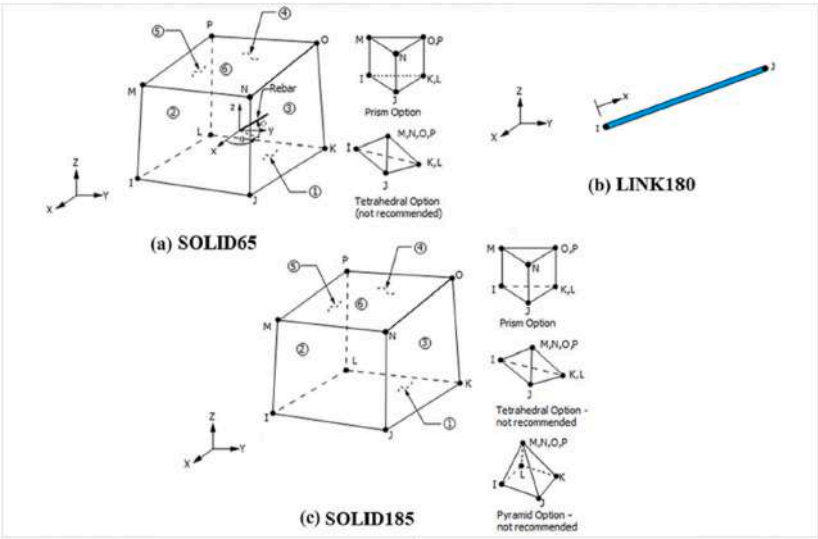

a)

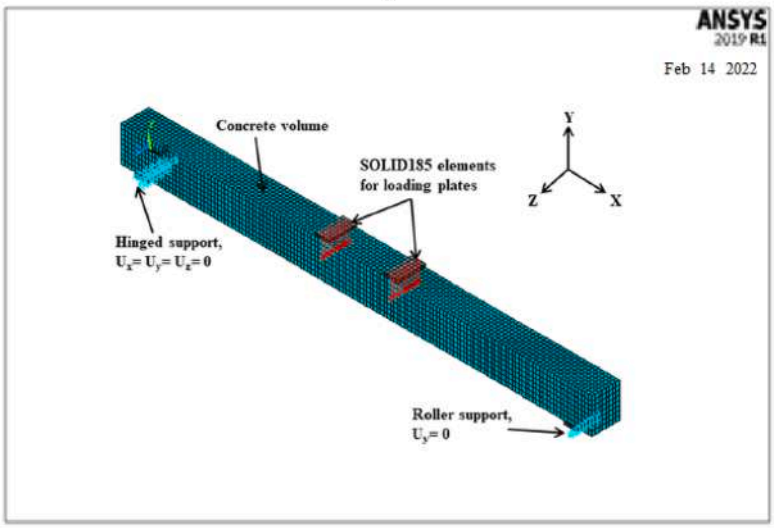

b)

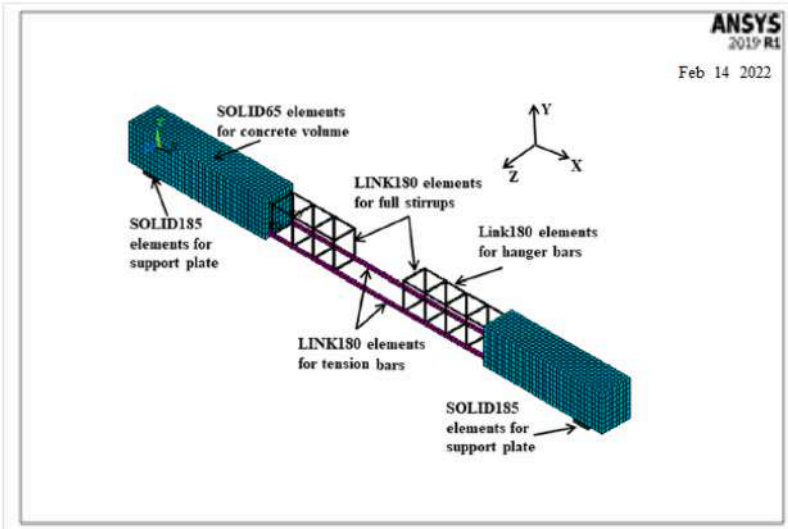

c)

(caption on next page)

Fig. 12. Representation of beam.

same as that used in the NLFEA.

Solid 65 is used for depicting the constituents of the experimentally tested beams. As indicated in Fig. 12, Link 180 spare was utilized to represent the reinforcing bars for steel and basalt bars.

4.1. Cracks pattern

Fig. 13 shows the NLFEA crack pattern for all modled beams which showed roughly comparable patterns of crack propagation in flexural failure. These cracks began in the center of the beams and progressed diagonally toward the loading locations.

4.2. NLFE ultimate load and corresponding deflection

Table 6 indicates the analytical ultimate loads for the beams and its corresponding deflections. The deflection was recorded using the obtained results from ANSYS results at the mid span verse to the corresponding experimental loads. It was observed that the load-deflection curves for specimens reinforced using hybrid GFRP bars was agreed with the behavior of experimental results. The maximum loads for control beams B1 and B2 are 41.26 kN and 53.13 kN, respectively, with deflections of 33.62 mm and 20.35 mm. The ultimate loads for beams B3, B4, B5, and B6 are 69.56 kN, 72.85 kN, 91.37 kN, and 98.70 kN, respectively. Their relative deflections are 27.82 mm, 29.14 mm, 36.55 mm, and 39.48 mm.

5. Comparison between experimental and NLFEA

In terms of ultimate load, ultimate deflection, and resulting ductility, six finite element models were compared to six experimental specimens.

5.1. Ultimate load

As indicated in Table 7 and Fig. 14-a, there is satisfactory agreement between the experimental and NLFEA failure loads. The $Pu_{NLFEA}/Pu_{exp.}$ ratios for beams B1, B2, and B3 were 0.90, 0.92, and 0.87, respectively. The $Pu_{NLFEA}/Pu_{exp.}$ ratios for beams B4, B5, and B6 were 0.89, 0.92, and 0.88, respectively. The NLFE analysis agreed well with the experimental data, with an average ratio of 0.90 in failure load. The average agreement between the NLFEA and experimental deflections was 0.90.

5.2. Ultimate deflections at ultimate load

Table 7 and Fig. (14-b) illustrate a comparison of experimental test deflection and NLFEA deflection. The concordance in behavior between the two obtained results was depicted in Fig. (13-b). The ratios of $\Delta ult_{NLFEA}/ult_{exp.}$ for beams B1, B2, and B3 deflection were 0.90, 0.92, and 0.87, respectively. The $\Delta ult_{NLFEA}/ult_{exp.}$ ratios for beams B4, B5, and B6 were 0.89, 0.92, and 0.88, respectively, indicating satisfactory agreement. The comparisons of experimental and NLFEA load deflection curves for all specimens are shown in Fig. 15. As a result of the preceding, the analytical models offered a satisfactory load deflection response.

5.3. Cracks pattern

The NLFEA crack pattern for all beams showed roughly comparable patterns of crack propagation in flexural failure. Fig. 16 shows a comparison of the results. These cracks began in the center of the beams and progressed diagonally toward the loading locations.

6. Conclusion

The current case study investigated at the flexural properties of RC beams reinforced with hybrid GFRP bars. This study demonstrates the advantages of hybrid GFRP bars in reinforcement over steel and conventional GFRP reinforcement. When the experimental data were compared to the values derived from analytical models, the following conclusions were reached:

1. The H-GFRP bars have the mechanical failure mechanism as reinforcement steel bars, which give the ductile failure mode when they reach their maximum capacity.
2. The load deflection curves for all H-GFRP beams demonstrated nearly complete model behavior with an increase in ductility.
3. The H-GFRP bars have adequate tensile strength and modulus of elasticity.

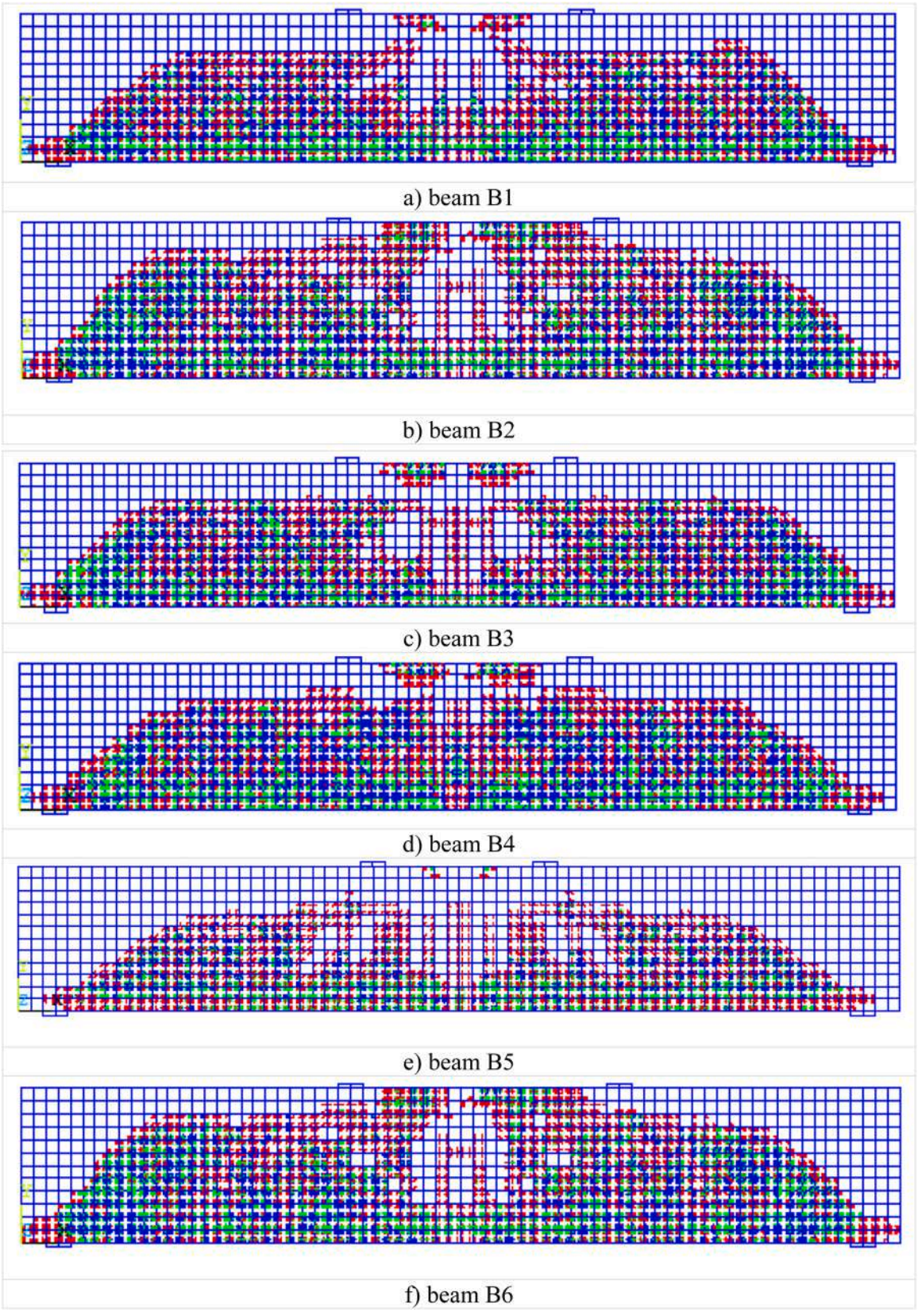

Fig. 13. Crack pattern for NLFE models.

Table 6
NLFEA results.

Specimen Id	1st crack load (kN)	Ultimate NLFE load (kN)	Deflection at 1st crack load, (mm)	Deflection at ultimate load, (mm)	Ductility index (%)
B1	2.5	41.26	0.45	33.62	16.50
B2	2.5	53.13	0.85	20.35	21.25
B3	2.5	69.56	1.25	11.68	27.82
B4	2.5	72.85	1.75	14.23	29.14
B5	2.5	91.37	0.55	20.07	36.55
B6	2.5	98.70	0.95	32.58	39.48

Table 7
Comparison between experimental and NLFEA.

Specimen Id	Exponential Load (kN)		Analytical Load (kN)		Deflection at ultimate load (mm)		$\frac{P(NLFE)}{P(Exp)}$		$\frac{\Delta u(NLFE)}{\Delta u(Exp)}$
	P 1st-crack	Pu	P 1st-crack	Pu	Δu_{Exp}	Δu_{NLFEA}	P 1st-crack	Pu	
B1	3.05	45.84	2.50	41.26	37.35	33.62	0.82	0.90	0.90
B2	5.40	57.75	2.50	53.13	22.12	20.35	0.46	0.92	0.92
B3	4.29	79.95	2.50	69.56	13.42	11.68	0.58	0.87	0.87
B4	2.53	81.85	2.50	72.85	16.00	14.23	0.99	0.89	0.89
B5	4.01	99.32	2.50	91.37	21.82	20.07	0.62	0.92	0.92
B6	5.17	112.16	2.50	98.70	37.02	32.58	0.48	0.88	0.88
Average							0.66	0.90	0.90
Variance							0.04	0.00	0.00
Standard Deviation							0.21	0.02	0.02

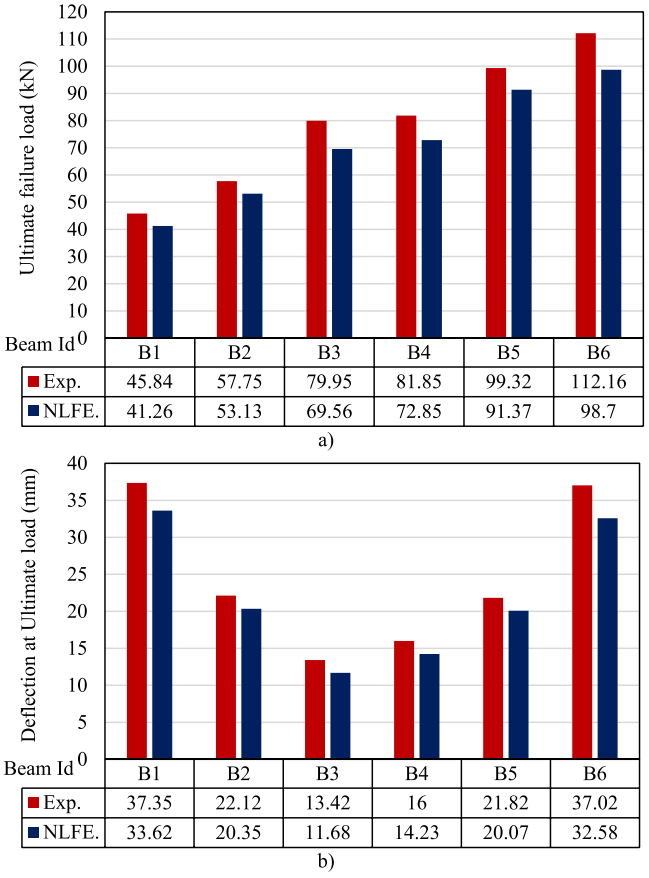

Fig. 14. Comparasions between experimental and NLFEA results; a) ultimate load; b) deflection at ultimate load.

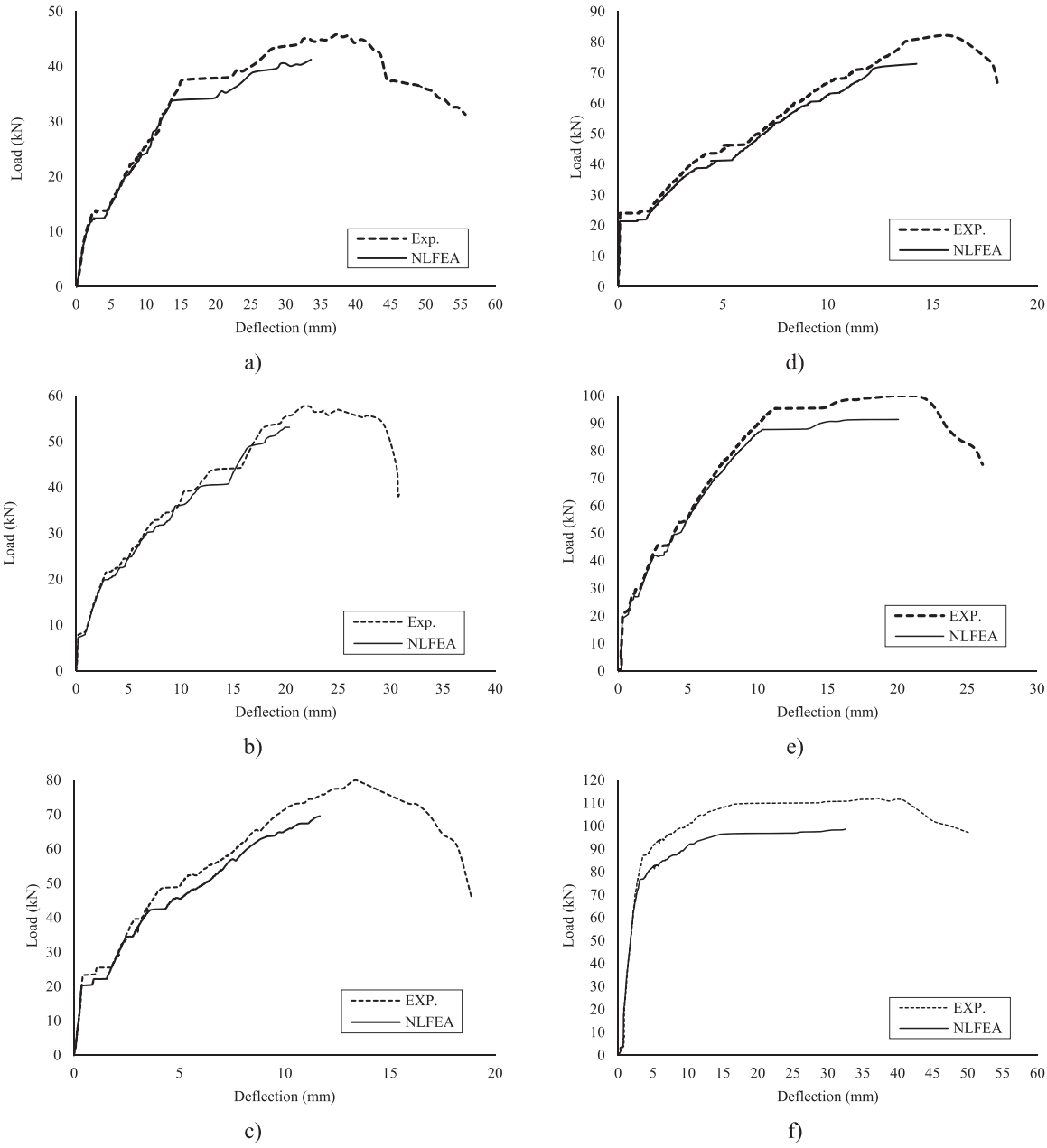

Fig. 15. Comparasions between experimental and NLFEA load-deflection curves; a) B1; b) B2; c) B3; d) B4; e) B5; f) B6.

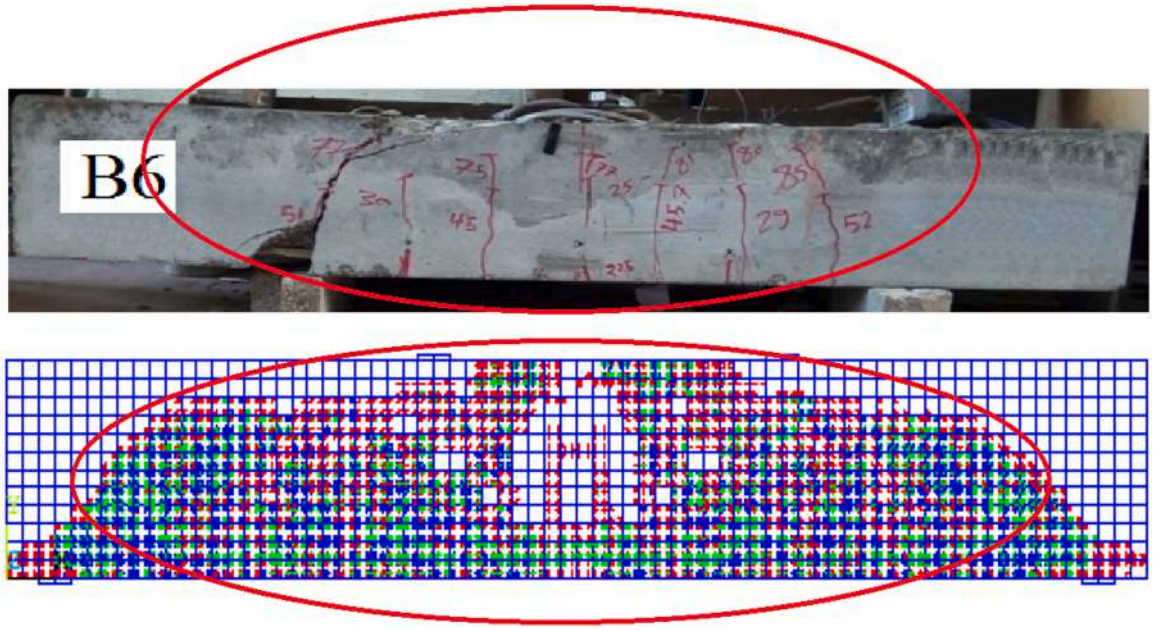

Fig. 16. Cracks pattern comparasions for beam B6.

4. The ultimate loads of beams with H-GFRP bars increased in comparison to beams reinforced with steel and ordinary GFRB bars. In the tested beams, the ratio of increase in ultimate load varies between 40% and 50%.
5. The H-GFRP beams ductulity index was improved when compared with conventional GFRP beams.
6. NLFEA with ANSYS 2019-R1 produces a computable result in terms of crack pattern, ultimate loads and deflection. $Pult_{NLFEA}$ / $Pult_{Exp}$ and Δult_{NLFE} / $\Delta ult_{Exp.}$ had average agreements of 0.90 and 0.90, respectively.

Declaration of Competing Interest

The authors declare that they have no known competing financial interests or personal relationships that could have appeared to influence the work reported in this paper.

References

[1] A.M. Erfan, H.E. Hassan, K.M. Hatab, T.A. El-Sayed, The flexural behavior of nano concrete and high strength concrete using GFRP, Constr. Build. Mater. 247 (2020), 118664.
[2] L. Heng, W. Zhou, W. Zhenyu, Flexural performance of concrete beams reinforced with FRP bars grouted in corrugated sleeves, Compos. Struct. 215 (2019) 49–59.
[3] D. Pawłowski, M. Szumigala, Flexural behavior of full-scale basalt FRP RC beams experimental and numerical studies, Procedia Eng. 108 (2015) 518–525.
[4] D. Tomlinson, A. Fam, Performance of concrete beams reinforced with basalt FRP for flexure and shear, J. Compos. Constr. 19 (2015) 1–10.
[5] D. Douglas, An Investigation into the Flexural Behavior of GFRP Reinforced Concrete Beams [MSc thesis], University of Toronto, Canada, 2012.
[6] Z. Soric, T. Kisicek, J. Galic, Deflections of concrete beams reinforced with FRP bars, Mater. Struct. 43 (2010) 73–90.
[7] M.K. Nassif, A.M. Erfan, O.T. Fadel, T.A. El-sayed, Flexural behavior of high strength concrete deep beams reinforced with GFRP bars, Case Stud. Constr. Mater. 15 (2021), e00613.
[8] G. Kretsis, "A review of the tensile, compressive, flexural and shear properties of hybrid fibre-reinforced plastics,", Composites Vol. 18 (No. 1) (1987) 13–23.
[9] A.M. Erfan, R.M. Abd Elnaby, A.A. Badr, T.A. El-sayed, Flexural behavior of HSC one way slabs reinforced with basalt FRP bars, Case Stud. Constr. Mater. 14 (2021), e00513.
[10] A.M. Erfan, Y.A. Algash, T.A. El-Sayed, Experimental and Analytical Behavior of HSC Columns Reinforced with Basalt FRP Bars, Int. J. Sci. Eng. Res. 10 (9) (2019) 240–260.
[11] T.A. El-Sayed, Performance of porous slabs using recycled ash, Polymers 13 (19) (2021) 3319.
[12] American Concrete Institute (ACI). (2015). "Guide for the Design and Construction of Concrete Reinforced with FRP Bars". ACI 440.1R-15, Farmington Hills, Mich.
[13] M. Habeeb, A.F. Ashour, Flexural behavior of continuous GFRP reinforced concrete beams, ASCE J. Compos. Constr. 12 (2) (2008) 115–124.
[14] A.M. Erfan, Y.A. Algash, T.A. El-Sayed, Experimental & Analytical Flexural Behavior of Concrete Beams Reinforced with Basalt Fiber Reinforced Polymers Bars, Int. J. Sci. Eng. Res. 10 (8) (2019) 297–315.
[15] M.A. Adam, A.M. Erfan, F.A. Habib, T.A. El-Sayed, Structural Behavior of High-Strength Concrete Slabs Reinforced with GFRP Bars, Polymers 13 (17) (2021) 2997.
[16] A. Nanni, M.J. Henneke, T. Okamoto, Tensile properties of hybrid rods for concrete reinforcement, Constr. Build. Mater. 8 (1) (1994) 27–34.
[17] R. Tepfers, V. Tamužs, R. Apinis, U. Vilks, J. Modniks, Ductility of nonmetallic hybrid fiber composite reinforcement for concrete, Mech. Compos. Mater. 32 (2) (1996) 113–121.
[18] W. Somboonsong, F.K. Ko, H.G. Harris, Ductile hybrid fiber reinforced plastic reinforcing bar for concrete structures: design methodology, Mater. J. 95 (6) (1998) 655–666.
[19] H.G. Harris, W. Somboonsong, F.K. Ko, New ductile hybrid FRP reinforcing bar for concrete structures, ASCE J. Compos. Constr. 2 (1) (1998) 28–37.

[20] B. Saikia, J. Thomas, A. Ramaswamy, K.N. Rao, Performance of hybrid rebars as longitudinal reinforcement in normal strength concrete, Mater. Struct. 38 (10) (2005) 857–864.
[21] (a) M.M. Cheung, T.K. Tsang, Behaviour of concrete beams reinforced with hybrid FRP composite rebar, Adv. Struct. Eng. 13 (1) (2010) 81–93 [11];
(b) Y. Cui, M.M. Cheung, B. Noruziaan, S. Lee, J. Tao, Development of ductile composite reinforcement bars for concrete structures, Mater. Struct. 41 (9) (2008) 1509–1518.
[22] E.E.-S. Etman, Innovative hybrid reinforcement for flexural members, ASCE J. Compos. Constr. 15 (1) (2010) 2–8.
[23] B. Behnam, C. Eamon, Analysis of alternative ductile fiberreinforced polymer reinforcing bar concepts, J. Compos. Mater. 48 (6) (2014) 723–733.
[24] Y. Zhou, Y. Wu, J. Teng, A. Leung, Ductility analysis of compression-yielding FRP-reinforced composite beams, Cement Concrete Compos. 31 (9) (2009) 682–691.
[25] S.H. Alsayed, A.M. Alhozaimy, Ductility of concrete beams reinforced with FRP bars and steel fibers, J. Compos. Mater. 33 (19) (1999) 1792–1806.
[26] V.C. Li, S. Wang, Flexural behaviors of glass fiber-reinforced polymer (GFRP) reinforced engineered cementitious composite beams, Mater. J. 99 (1) (2002) 11–21.
[27] H. Wang, A. Belarbi, Ductility characteristics of fiberreinforced- concrete beams reinforced with FRP rebars, Constr. Build. Mater. 25 (5) (2011) 2391–2401.
[28] Tan, K. H. (1997) Behaviour of hybrid FRP-steel reinforced concrete beams. Proc., 3rd Int. Symp. on Non-Metallic (FRP) Reinforcement for Concrete Structures (FRPRCS-3), Japan Concrete Institute, Tokyo, 487–494.
[29] M.A. Aiello, L. Ombres, Structural performances of concrete beams with hybrid (fiber-reinforced polymer-steel) reinforcements, ASCE J. Compos. Constr. 6 (2) (2002) 133–140.
[30] H. Leung, R. Balendran, Flexural behaviour of concrete beams internally reinforced with GFRP rods and steel rebars, Struct. Survey 21 (4) (2003) 146–157.
[31] W. Qu, X. Zhang, H. Huang, Flexural behavior of concrete beams reinforced with hybrid (GFRP and steel) bars, ASCE J. Compos. Constr. 13 (5) (2009) 350–359.
[32] W. Qu, X. Zhang, H. Huang, Flexural behavior of concrete beams reinforced with hybrid (GFRP and steel) bars, J. Compos. Constr. 13 (2009) 350–359.
[33] S. Zeyang, F. Linchen, D.F. Cheng, A.R. Vatuloka, W. Yang, Experimental study on the flexural behavior of concrete beams reinforced with bundled hybrid steel/FRP bars, Eng. Struct 197 (2019) 1–10.
[34] A. El-Refai, F. Abed, A. Al-Rahmani, Structural performance and serviceability of concrete beams reinforced with hybrid (GFRP and steel) bars, Constr. Build. Mater. 96 (2015) 518–529.
[35] W. Ge, J.D. Zhang, C. Dafu, T. Yongming, Flexural behaviors of hybrid concrete beams reinforced with BFRP Bars and steel bars, Constr. Build. Mater. 87 (2015) 28–37.
[36] I.F. Kara, A.F. Ashour, M.A. Koroğlu, Flexural behavior of hybrid FRP/steel reinforced concrete beams, Compos. Struct. 129 (2015) 111–121.
[37] M.A. Safan, Flexural behavior and design of steel–GFRP reinforced concrete beams, ACI Mater. J. 110 (6) (2013) 677–685.
[38] D. Lau, H.J. Pam, Experimental study of hybrid FRP reinforced concrete beams, Eng. Struct. 32 (12) (2010) 3857–3865.
[39] M.A. Aiello, L. Ombres, Structural performances of concrete beams with hybrid reinforcements, J. Compos. Constr. 6 (2) (2002) 133–140.
[40] H.Y. Leung, R.V. Balendran, Flexural behavior of concrete beams internally reinforced with GFRP rods and steel bars, Struc. Surv 21 (2003) 146–157.
[41] J. Minkwan, L. Sangyun, C. Park, Response of glass fiber reinforced polymer (GFRP)- steel hybrid reinforcing bar in uniaxial tension, Int J Concr. Struct. Mater. 11 (2017) 677–686.
[42] U. Priyanka, M. Siva, Hybrid reinforcement by using GFRP, Int. Res. J. Eng. Technol. 3 (2016) 642–645.
[43] Park KT, Hyeong YK, Young JY, Sang YL, Dong WS. Hybrid FRP reinforcing bars for concrete structures. Fourth Asia-Pacific Conference on FRP in Structures, International Institute for FRP in Construction. 2013.
[44] E. Etman, Flexural performance of RC slabs with internal hybrid reinforcement, 5th IECC'5, American Society of Civil Engineers, 2008.
[45] T.A. El-Sayed, Y.A. Algash, Flexural behavior of ultra-high performance geopolymer RC beams reinforced with GFRP bars, Case Stud. Constr. Mater. (2021), e00604.
[46] ANSYS," Engineering Analysis system user's Manual" 2005, vol. 1&2, and theoretical manual. Revision 8.0, Swanson analysis system inc., Houston, Pennsylvania.